

# MERGING EXTREMUM SEEKING AND SELF-OPTIMIZING NARROWBAND INTERFERENCE CANCELLER – OVERDETERMINED CASE

*Michał Meller*

Department of Automatic Control, Faculty of Electronics, Telecommunications and Computer Science,  
Gdańsk University of Technology, Narutowicza 11/12, 80-233 Gdańsk, Poland,  
e-mail: [michal.meller@eti.pg.gda.pl](mailto:michal.meller@eti.pg.gda.pl)

## ABSTRACT

Active cancellation systems rely on destructive interference to achieve rejection of unwanted disturbances entering the system of interest. Typical practical applications of this method employ a simple single input, single output arrangement. However, when a spatial wavefield (e.g. acoustic noise or vibration) needs to be controlled, multichannel active cancellation systems arise naturally. Among these, the so-called overdetermined control configuration, which employs more measurement outputs than control inputs, is often found to provide superior performance.

The paper proposes an extension of the recently introduced control scheme, called self-optimizing narrowband interference canceller (SONIC), to the overdetermined case. The extension employs a novel variant of the extremum-seeking adaptation loop which uses random, rather than sinusoidal, probing signals. This modification simplifies design of the controller and improves its convergence. Simulations, performed using a realistic model of the plant, demonstrate improved properties of the new controller.

**Index Terms**— extremum seeking, disturbance rejection, adaptive control, active noise control,

## 1. INTRODUCTION

Narrowband disturbances, such as vibration and acoustic noise, often arise in rotating mechanical systems. In the range of high frequencies these disturbances may be eliminate by traditional, passive, means. Typical examples of the passive approach include screens, dampeners or absorbers.

Unfortunately, these well established measures often fail at low frequencies. This is because their physical dimensions and mass are related to the wavelength of the disturbances they are to cope with. Simply put, to work well in the low frequency range, passive solutions must be so large and heavy that they are no longer attractive.

However, low frequency disturbances can be cancelled using active methods, which are based on the principle of de-

structive interference. Vaguely speaking [1], the idea behind the active approach is to generate a control signal such that, at the point or area of interest, has amplitude equal to that of the disturbance, but “opposite” (i.e. displaced by  $\pi$ ) phase.

Multivariate active control systems gain particular relevance when the volume of the area of interest becomes large. This is because, to exert proper control of a large acoustic/vibration wavefield, it is desirable to both act and take measurements at multiple locations.

Depending on the relative numbers of control inputs  $M$  and measurement outputs  $N$  multivariate active control systems can be divided into three basic configurations: the so-called undetermined case ( $M > N$ ), the fully determined case ( $M = N$ ) and the overdetermined case ( $M < N$ ). Practical experience suggests that the overdetermined configuration allows one to obtain the best control results [1]. This is because, in the first two cases, an improper placement of the sensors might cause the *local* control results to give an *illusion* of very good performance. However, the true, spatially averaged, performance may be unsatisfactory. On the other hand, if an “excessive” number of sensors is employed, such a situation is considerably less likely to occur.

The majority of existing active control solutions, of which the FX-LMS algorithm [1] is the most important one, share a common limitation – they require one to know the transfer function of the controlled plant. In case when the plant is unknown or time-varying they must be extended with means of on-line plant estimation (see e.g. [2]). However, since the estimation process is carried out in a closed loop, identifiability problems are not unlikely to occur. These may cause the plant estimate may to become biased [3] which adversely affects performance.

In our recent papers we proposed a novel approach to active control, free of the above difficulty. The method, initially introduced for the known frequency, single input single output case [4], was later extended in a number of ways, including the time varying frequency [5] and the multiple input multiple output [3] cases.

Real world experience with the SONIC controller allowed us to identify its two, potentially weak, points. First, the self-optimization loop of the algorithm may not provide enough

---

This work was supported by the National Science Centre under grant no. UMO-2011/03/B/ST7/01882.

robustness against nonlinear dynamics or large transport delays. Second, the multivariate version of the algorithm does not extend to the overdetermined case.

To cope with the first issue we proposed a modified self-optimization loop [6], based on the extremum seeking (ES) approach [7]. The modified loop proved substantially more robust than the standard one.

Here we tackle the second problem. We propose an overdetermined variant of the SONIC controller. The solution is, again, based on extremum seeking. However, unlike [6] and [7], the new scheme employs random, rather than sinusoidal, probing signal. This modification simplifies the design of the control system considerably and makes it more robust against the influence of the narrowband disturbance.

The paper is organized as follows. Section 2 states the overdetermined active control problem. In section 3 the proposed controller is introduced. Its analysis is carried out in section 4. Section 5 presents simulation results.

## 2. PROBLEM STATEMENT

Consider the system governed by the following equation

$$\mathbf{y}(t) = \mathbf{K}_P(q^{-1})\mathbf{u}(t-1) + \mathbf{d}(t) + \mathbf{v}(t), \quad (1)$$

where  $t$  denotes discrete time,  $q^{-1}$  is the backward-shift operator,  $q^{-1}\mathbf{u}(t) = \mathbf{u}(t-1)$ ,  $\mathbf{y}(t)$  denotes the  $N$ -dimensional system output,  $\mathbf{u}(t)$  is the  $M$ -dimensional system input,

$$\begin{aligned} \mathbf{d}(t) &= \mathbf{a}e^{j\omega_0 t} \\ \mathbf{a} &= [a_1 e^{j\phi_1} \ a_2 e^{j\phi_2} \ \dots \ a_N e^{j\phi_N}]^T \end{aligned} \quad (2)$$

is the  $N$ -dimensional vector of narrowband disturbances with complex amplitudes  $a_1, a_2, \dots, a_N$ , initial phases  $\phi_1, \phi_2, \dots, \phi_N$  and known frequency  $\omega_0$ ,  $\mathbf{v}(t)$  denotes the wideband disturbance and

$$\mathbf{K}_P(q^{-1}) = \begin{bmatrix} K_{11}(q^{-1}) & K_{12}(q^{-1}) & \dots & K_{1M}(q^{-1}) \\ \vdots & \vdots & \ddots & \vdots \\ K_{N1}(q^{-1}) & K_{N2}(q^{-1}) & \dots & K_{NM}(q^{-1}) \end{bmatrix} \quad (3)$$

is the  $N \times M$  transfer function matrix of the  $M$ -input,  $N$ -output unknown linear stable plant.

In the sequel we will focus our attention on the overdetermined case,  $N > M$ . We will seek for a minimum-variance controller, i.e. controller allowing one to minimize the following cost function

$$J = \lim_{t \rightarrow \infty} E[\mathbf{y}^H(t)\mathbf{y}(t)]. \quad (4)$$

Note that, in contrast to our previous work [3], when  $N > M$  perfect (or nearly perfect) cancellation is not possible – unless the disturbance happens to lie in the image space of the plant. This limitation holds even when the wideband noise is absent,  $\mathbf{v}(t) \equiv \mathbf{0}$ .

## 3. PROPOSED SOLUTION

### 3.1. Multivariate SONIC for the overdetermined case

The multivariate version of the SONIC controller, in its original form, applies to the fully determined case only. It takes the form [3]

$$\begin{aligned} \tilde{\mathbf{z}}(t) &= e^{j\omega_0}[(1 - c_\mu)\tilde{\mathbf{z}}(t-1) - c_\mu\mathbf{y}(t-1)] \\ \widehat{\mathbf{M}}(t) &= \widehat{\mathbf{M}}(t-1)[\mathbf{I} - \alpha\mathbf{y}(t)\tilde{\mathbf{z}}^H(t)] \\ \widehat{\mathbf{d}}(t+1|t) &= e^{j\omega_0}[\widehat{\mathbf{d}}(t|t-1) + \widehat{\mathbf{M}}(t)\mathbf{y}(t)] \\ \mathbf{u}(t) &= -\mathbf{k}_N^{-1}\widehat{\mathbf{d}}(t+1|t), \end{aligned} \quad (5)$$

where  $\widehat{\mathbf{d}}(t+1|t)$  denotes the one step ahead disturbance prediction,  $\mathbf{k}_N$  is the complex gain of the nominal (assumed) plant at the frequency  $\omega_0$ ,  $\mathbf{k}_N = \mathbf{K}_N(e^{-j\omega_0})$ , typically obtained from a separate off-line plant identification experiment,  $\widehat{\mathbf{M}}(t)$  is the  $N \times N$  matrix of complex estimation gains and  $\tilde{\mathbf{z}}(t)$  is the estimate of the gradient of the cost function.

The algorithm consists of two loops. The inner loop – the last two equations of (5) – predicts the disturbance and, using the nominal model  $\mathbf{k}_N$ , works out a suitable cancelling signal. However, since the nominal plant may differ from the true one,  $\mathbf{K}_N(e^{-j\omega_0}) \neq \mathbf{K}_P(e^{-j\omega_0})$ , the outer, self-optimization, loop is necessary to guarantee proper performance. This loop recursively adjusts the complex gain matrix  $\widehat{\mathbf{M}}(t)$  so, as to: 1. Compensate modeling errors, 2. Adjust the convergence rate of the closed loop system to match the nonstationarity rate of the plant and/or disturbance.

A naïve extension of the control loop of (5) to the overdetermined case could take the following form

$$\begin{aligned} \widehat{\mathbf{d}}(t+1|t) &= e^{j\omega_0}[\widehat{\mathbf{d}}(t|t-1) + \widehat{\mathbf{M}}(t)\mathbf{y}(t)] \\ \mathbf{u}(t) &= -\mathbf{k}_N^\# \widehat{\mathbf{d}}(t+1|t), \end{aligned} \quad (6)$$

where  $\widehat{\mathbf{M}}(t) \in \mathcal{C}_{N \times N}$  and  $\mathbf{k}_N^\# \in \mathcal{C}_{M \times N}$  denotes the pseudoinverse of  $\mathbf{k}_N$ . However, such a form of the control part has one serious drawback. Under  $\widehat{\mathbf{M}}(t) = \mathbf{M} = \text{const}$ , it holds that the control signal is governed by

$$\mathbf{u}(t) = -\mathbf{K}_C(q^{-1})\mathbf{y}(t), \quad (7)$$

where the controller's MIMO transfer function  $\mathbf{K}_C(q^{-1})$  takes the form

$$\begin{aligned} \mathbf{K}_C(q^{-1}) &= [1 - e^{j\omega_0}q^{-1}]^{-1}e^{j\omega_0}\mathbf{G}_{\text{eff}} \\ \mathbf{G}_{\text{eff}} &= \mathbf{k}_N^\# \mathbf{M}. \end{aligned} \quad (8)$$

Observe that the effective gain matrix  $\mathbf{G}_{\text{eff}}$  has the dimension  $M \times N$ , while  $\mathbf{M}$  is a larger  $N \times N$  matrix. This means that, had (6) been used, the resulting adaptive controller would suffer from overparametrization – there exist an infinite number of matrices  $\mathbf{M}$  which could yield the same  $\mathbf{G}_{\text{eff}}$ . This could potentially lead to an undesirable behavior, e.g. bursting.

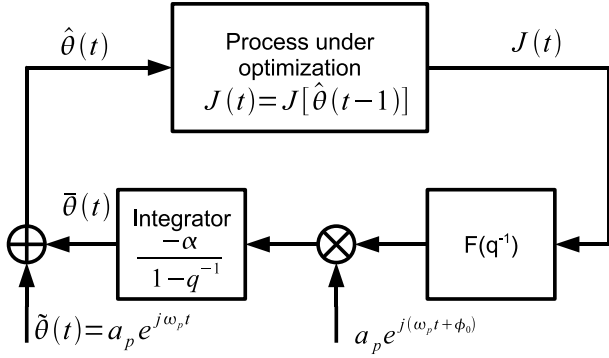


**Fig. 1.** Block diagram of the conventional extremum seeking loop which uses sinusoidal probing signals.

Keeping this in mind, we will adopt the following control loop

$$\mathbf{u}(t) = e^{j\omega_0} [\mathbf{u}(t-1) - \hat{\mathbf{G}}(t)\mathbf{y}(t)], \quad (9)$$

where  $\hat{\mathbf{G}}(t) \in \mathcal{C}_{M \times N}$  denotes the time varying gain matrix.

In the following subsections a new self-optimization loop will be designed for (5). Similar to [6], it will be founded on the extremum seeking approach, which offers a great deal of robustness [7].

### 3.2. Extremum seeking using random probing signals

Fig. 1 depicts the conventional extremum seeking system. It is assumed that the output of the process is the minimized cost function  $J(t) = J[\boldsymbol{\theta}(t-1)]$ , where  $\boldsymbol{\theta}(t) = [\theta_1 \theta_2 \dots \theta_K]^T$  is the vector of the adapted variables. To estimate the gradient of the cost function, the ES loop injects sinusoidal perturbation signals into  $\boldsymbol{\theta}(t)$  and applies special processing to the process output. Finally, since  $J(t)$  is minimized,  $\boldsymbol{\theta}(t)$  is adjusted in the direction opposite to the estimated gradient using the integrator block [7].

The conventional approach has one drawback – in the multivariate case the frequencies of the sinusoidal perturbation signals must be chosen with a great deal of care. Since the cost function is usually nonlinear in parameters, the sinusoidal perturbation signal will give rise to multiple spectral components in  $J(t)$ . The frequencies of these components will be equal to various sums/differences of the probing signals frequencies. Unless all these spectral components are well separated from each other, individual ES loops may interact with each other, leading to unsatisfactory convergence. This separation condition becomes increasingly more difficult to satisfy when the number of adapted parameters becomes large, as is the case of active noise/vibration control.

To cope with this issue we propose to employ a modified version of the extremum seeking loop which uses complex random probing signals.

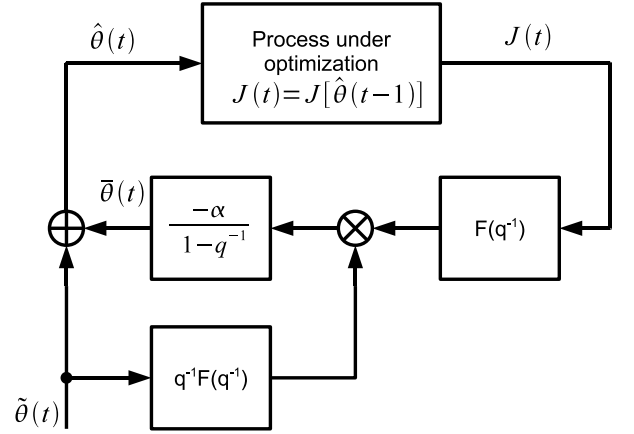


**Fig. 2.** Block diagram of the modified extremum seeking loop which employs complex random probing signals.

The block diagram of the modified approach is shown in Fig. 2. The sinusoidal signals were replaced with a complex random vector  $\tilde{\boldsymbol{\theta}}(t)$ . The filter  $F(q^{-1})$  plays two roles. First, it removes the DC component of  $J$ , which conveys no useful information. Second, it filters out measurement noise. The gradient of the cost function is sensed by means of correlation processing of the filtered process output and the filtered probing signal. Finally, the vector  $\bar{\boldsymbol{\theta}}(t)$  is adapted in the direction opposite to the estimated gradient.

### 3.3. Theoretical analysis

The proposed extremum seeking loop can be summarized using the following equations

$$\begin{aligned} \bar{\boldsymbol{\theta}}(t) &= \bar{\boldsymbol{\theta}}(t-1) - \alpha \tilde{\boldsymbol{\theta}}_f(t) J_f(t) \\ \tilde{\boldsymbol{\theta}}_f(t) &= F(q^{-1}) \tilde{\boldsymbol{\theta}}(t-1) \\ J_f(t) &= F(q^{-1}) J[\boldsymbol{\theta}(t-1)] \\ \boldsymbol{\theta}(t) &= \bar{\boldsymbol{\theta}}(t) + \tilde{\boldsymbol{\theta}}(t). \end{aligned} \quad (10)$$

Under slow adaptation,  $\alpha \cong 0$ , the stochastic averaging approach may be applied in the analysis of (10). Then (10) is replaced with

$$\bar{\boldsymbol{\theta}}(t) = \bar{\boldsymbol{\theta}}(t-1) - \alpha E[\tilde{\boldsymbol{\theta}}_f(t) J_f(t; \bar{\boldsymbol{\theta}}(t-1))], \quad (11)$$

where  $E[\cdot]$  denotes the expected value and  $J_f(t; \bar{\boldsymbol{\theta}}(t-1))$  denotes the stationary stochastic process which settles down for a constant value of  $\bar{\boldsymbol{\theta}}(t)$ .

To move ahead we need the following assumption:

**(A1)** The function  $J[\boldsymbol{\theta}(t-1)]$  is differentiable in the complex-real (CR) sense [8] around  $\bar{\boldsymbol{\theta}}(t-1)$ .

When (A1) holds, one is allowed to apply a Taylor-style expansion of  $J[\boldsymbol{\theta}(t-1)]$  around  $\bar{\boldsymbol{\theta}}(t-1)$ , which takes the

form

$$J[\boldsymbol{\theta}(t-1)] \cong J[\bar{\boldsymbol{\theta}}(t-1)] + \bar{\boldsymbol{\theta}}^T(t-1) \frac{\partial J}{\partial \boldsymbol{\theta}} + \bar{\boldsymbol{\theta}}^H(t-1) \frac{\partial J}{\partial \boldsymbol{\theta}^*}, \quad (12)$$

where  $\partial J/\partial \boldsymbol{\theta}$ ,  $\partial J/\partial \boldsymbol{\theta}^*$ , both evaluated at  $\bar{\boldsymbol{\theta}}(t-1)$ , are defined as

$$\begin{aligned} \frac{\partial J}{\partial \boldsymbol{\theta}} &= \left[ \frac{\partial J}{\partial \theta_1} \quad \frac{\partial J}{\partial \theta_2} \quad \cdots \quad \frac{\partial J}{\partial \theta_K} \right]^T \\ \frac{\partial J}{\partial \boldsymbol{\theta}^*} &= \left[ \frac{\partial J}{\partial \theta_1^*} \quad \frac{\partial J}{\partial \theta_2^*} \quad \cdots \quad \frac{\partial J}{\partial \theta_K^*} \right]^T \end{aligned} \quad (13)$$

and

$$\begin{aligned} \frac{\partial}{\partial \theta_i} &= \frac{1}{2} \left[ \frac{\partial}{\partial \text{Re } \theta_i} - j \frac{\partial}{\partial \text{Im } \theta_i} \right] \\ \frac{\partial}{\partial \theta_i^*} &= \frac{1}{2} \left[ \frac{\partial}{\partial \text{Re } \theta_i} + j \frac{\partial}{\partial \text{Im } \theta_i} \right]. \end{aligned} \quad (14)$$

Following [8], the steepest descent direction for adjusting  $\bar{\boldsymbol{\theta}}(t)$  is opposite to  $\partial J/\partial \boldsymbol{\theta}^*$ . We will show that, under the following additional assumption

**(A2)** The probing signal  $\tilde{\boldsymbol{\theta}}(t)$  is a zero mean, wide-sense stationary circular Gaussian white noise with power spectral density matrix

$$\mathbf{S}_{\tilde{\boldsymbol{\theta}}\tilde{\boldsymbol{\theta}}}(\omega) = \sum_{\tau=-\infty}^{\infty} \mathbf{E} \left[ \tilde{\boldsymbol{\theta}}(t) \tilde{\boldsymbol{\theta}}^H(t-\tau) \right] e^{-j\omega\tau} = S(e^{-j\omega}) \mathbf{I} \quad (15)$$

it holds that  $\mathbf{E}[\tilde{\boldsymbol{\theta}}_f(t) J_f(t; \bar{\boldsymbol{\theta}}(t-1))]$  is, up to a positive scale factor, proportional to  $\partial J/\partial \boldsymbol{\theta}^*$ .

Indeed, combining (10), (12) and (A2) leads to the following result

$$\begin{aligned} &\mathbf{E}[\tilde{\boldsymbol{\theta}}_f(t) J_f(t; \bar{\boldsymbol{\theta}}(t-1))] \\ &= \mathbf{E} \left\{ \tilde{\boldsymbol{\theta}}_f(t) \left[ F(q^{-1}) J[\bar{\boldsymbol{\theta}}(t-1)] + \bar{\boldsymbol{\theta}}_f^T(t) \frac{\partial J}{\partial \boldsymbol{\theta}} + \bar{\boldsymbol{\theta}}_f^H(t) \frac{\partial J}{\partial \boldsymbol{\theta}^*} \right] \right\} \\ &= 0 + \mathbf{E}[\tilde{\boldsymbol{\theta}}_f(t) \tilde{\boldsymbol{\theta}}_f^T(t)] \frac{\partial J}{\partial \boldsymbol{\theta}} + \mathbf{E}[\tilde{\boldsymbol{\theta}}_f(t) \tilde{\boldsymbol{\theta}}_f^H(t)] \frac{\partial J}{\partial \boldsymbol{\theta}^*} \\ &= \mathbf{E}[\tilde{\boldsymbol{\theta}}_f(t) \tilde{\boldsymbol{\theta}}_f^H(t)] \frac{\partial J}{\partial \boldsymbol{\theta}^*} \end{aligned} \quad (16)$$

where the last transition stems from circularity of  $\tilde{\boldsymbol{\theta}}(t)$ . Finally, since

$$\begin{aligned} \mathbf{E}[\tilde{\boldsymbol{\theta}}_f(t) \tilde{\boldsymbol{\theta}}_f^H(t)] &= \int_{\omega=0}^{2\pi} |F(e^{-j\omega})|^2 \mathbf{S}_{\tilde{\boldsymbol{\theta}}\tilde{\boldsymbol{\theta}}}(e^{-j\omega}) d\omega \\ &= \int_{\omega=0}^{2\pi} |F(e^{-j\omega})|^2 S(e^{-j\omega}) \mathbf{I} d\omega = C \mathbf{I}, \end{aligned} \quad (17)$$

where  $C$  is a positive constant, one obtains that

$$\mathbf{E}[\tilde{\boldsymbol{\theta}}_f(t) J_f(t; \bar{\boldsymbol{\theta}}(t-1))] = C \frac{\partial J}{\partial \boldsymbol{\theta}^*}. \quad (18)$$

This shows that the proposed adaptation mechanism correctly estimates the optimal update direction.

**Remark:** Note that the assumption that the filter  $F(q^{-1})$  has zero at DC,  $F(1) = 0$  is not necessary. However, removing the DC component of  $J[\boldsymbol{\theta}(t)]$  is beneficial, because it reduces the variance of the term  $\tilde{\boldsymbol{\theta}}_f(t) J_f(t; \bar{\boldsymbol{\theta}}(t-1))$  considerably.

## 4. SIMULATION RESULTS

The simulated control system configuration consists of two loops. The inner loop is composed of the controller (9) and the 2 input - 3 output, linear stable plant. Impulse responses of the plant were obtained from a real world active vibration control device and included features which can make control problem difficult, e.g. transport delay and poorly damped pole/zero pairs. The disturbance signal took the form (2) with  $\mathbf{a} = [1 \ 0.5 \ 1]^T$  and  $\omega_0 = 1.88$  rad/Sa. The outer loop, based on extremum seeking, adjusts the gain matrix  $\hat{\mathbf{G}}(t)$  of the inner loop.

Note that the inner loop is of dynamic nature. This means that any changes of  $\hat{\mathbf{G}}(t)$  take time to appear at the process output. Furthermore, since the dynamics of the inner loop are unknown (due to the plant itself being unknown), this delay cannot be easily compensated. However, the following simple solution was found to be very effective. To make the plant appear more static, the ES loop operates with a slower rate than the control loop. A single period of the ES loop, further referred to as the ‘epoch’, consisted of  $T = 50$  plant sampling periods. The cost criterion takes the form

$$J[\boldsymbol{\theta}(n)] = \sum_{\tau=0}^{T-1} \mathbf{y}^H(nT + \tau) \mathbf{y}(nT + \tau), \quad (19)$$

where  $n$  denotes the epoch index.

The probing signal was generated as a complex circular Gaussian white noise with covariance matrix equal to  $\sigma^2 \mathbf{I}$ , where  $\sigma = 0.005 \|\hat{\mathbf{G}}(t)\|_F$  and  $\|\cdot\|_F$  denotes the Frobenius norm.

The remaining settings for the ES loop were simple:  $\alpha = 1$ ,  $F(q^{-1}) = (1 - q^{-1})/(1 - 0.9q^{-1})$ .

To avoid erratic start, the control loop was initialized with  $\hat{\mathbf{G}}(0) = 0.02 \mathbf{k}_N^\#$ . To make the simulation realistic, each element of the nominal model matrix  $\mathbf{k}_N$  featured random multiplicative perturbation with standard deviation equal to 30% of the corresponding element of the true plant’s complex gain matrix  $\mathbf{k}_P$ .

During the first 2500 samples, the ES loop was disabled. This period plays the role of the reference. Between  $t = 2501$  and  $t = 3500$ , the probing signal was generated, but the update was not performed. Finally, at  $t = 3501$  the ES loop was allowed to be fully operational.

Fig. 3 shows the evaluated values of the cost criterion during the experiment. Observe the almost two-fold improvement after the ES loop has been enabled.

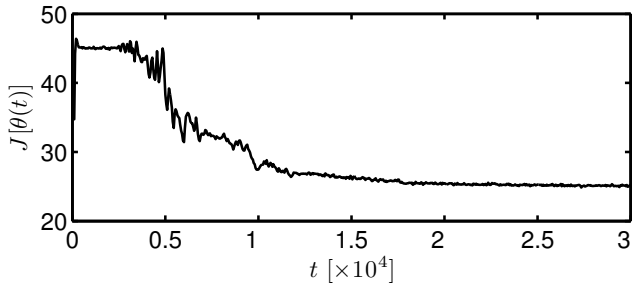


Fig. 3. Behavior of the cost criterion during the simulation experiment.

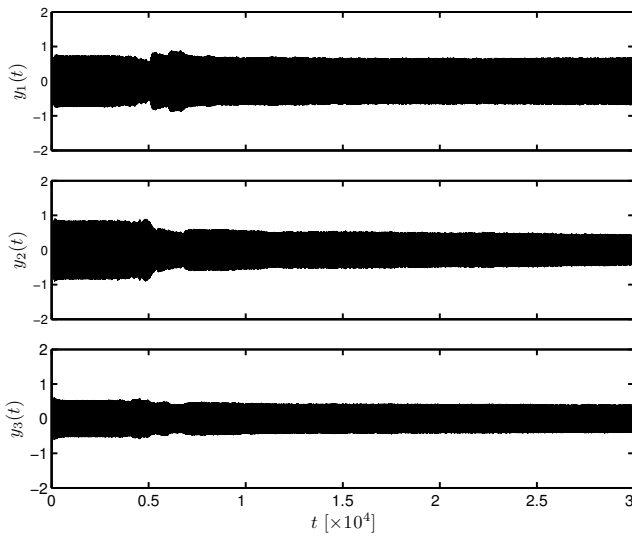


Fig. 4. Closed loop system outputs during the simulation experiment.

The corresponding output signals are shown in Fig. 4. Clearly, most of the improvement was found at the second output. However, note that, with an exception of the transient phase, the performance in the first output was not affected adversely. Finally, a small improvement was also obtained at the third output.

Fig. 5 depicts the closed loop system outputs when the algorithm from [3], developed for the fully determined case, was used in place of the proposed one. Obviously, in this case only two of the three plant's outputs could be used for the control purposes. Observe that, while the disturbance appears nearly canceled at these two outputs, its level is significantly elevated at the third one. This means that the control strategy was not successful, because the wavefield was cancelled only locally. On the other hand, the proposed solution yields a better overall performance, because a "global" improvement was reached.

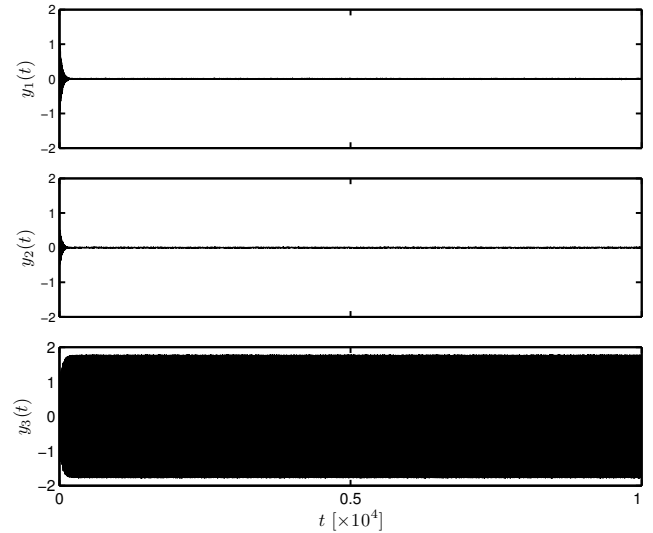


Fig. 5. Closed loop system outputs obtained using control algorithm developed for the fully determined case.

- [1] S. M. Kuo and D. Morgan, *Active Noise Control Systems: Algorithms and DSP Implementations*, Wiley, New York, 1995.
- [2] L. J. Eriksson and M. C. Allie, "Use of random noise for on-line transducer modeling in an adaptive active attenuation system," *J. Acoust. Soc. Am.*, vol. 85, pp. 797–802, Feb. 1989.
- [3] M. Meller and M. Niedźwiecki, "Multichannel self-optimizing narrowband interference canceller," *Signal Processing*, vol. 98, pp. 396–409, 2014.
- [4] M. Niedźwiecki and M. Meller, "A new approach to active noise and vibration control - part 1: the known frequency case," *IEEE Transactions on Signal Processing*, vol. 57, no. 9, pp. 3373–3386, 2009.
- [5] M. Niedźwiecki and M. Meller, "Hybrid SONIC: joint feedforward-feedback narrowband interference canceler," *International Journal of Adaptive Control And Signal Processing*, vol. 27, no. 12, pp. 1048–1064, 2013.
- [6] M. Meller and M. Niedźwiecki, "Robustification of the self-optimizing narrowband interference canceler – extremum seeking in complex domain," in *Proc. 2012 IEEE 51st Annual Conference on Decision and Control*, 2012, pp. 4805–4810.
- [7] K. B. Ariyur and Miroslav Krstić, *Real-Time Optimization by Extremum Seeking Feedback*, Wiley, 2003.
- [8] A. van den Bos, "Complex gradient and Hessian," *IEE Proc. Image Signal Processing*, vol. 141, pp. 380–382, 1994.

## REFERENCES